

Electronic supplementary information

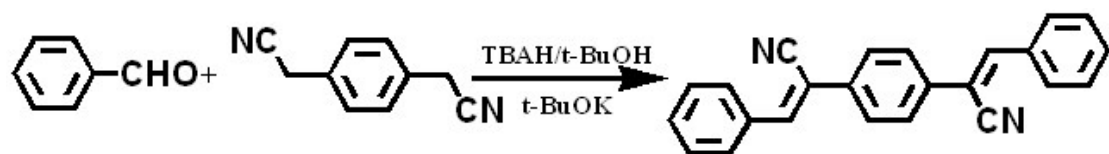
Fluorescent mutation and structural evolution of a  $\pi$ -conjugated molecular crystal as phase transition

*Yuanxiang Xu, Kai Wang, Yujian Zhang, Zengqi Xie, Bo Zou\* and Yuguang Ma\**

Table of Content:

1. Synthesis of CN-DSB. ....	S2
2. Photograph of CN-DSB crystals in the growth tube. ....	S2
3. PL spectra of blue and green CN-DSB crystal . ....	S3
4. Crystal data and structure refinement. ....	S3
5. Discussion on PL spectra of blue CN-DSB crystal as increasing the pressure. ....	S4
6. PL spectra of blue CN-DSB crystal as decreasing the pressure . ....	S5
7. In situ angle dispersive X-ray diffraction (ADXRD) patterns at varied pressures . ....	S5
8. Pressure-dependent of the intensity ratio $I_{\text{phenyl}} / I_{\text{vinylene}}$ . ....	S6
9. Powder XRD patterns of CN-DSB. ....	S6
10. FT-IR spectra at room temperature for B-phase and G-phase . ....	S7
11. Schematic illustration for the FsLDW fabrication of raster. ....	S7
12. The details of FsLDW experiment . ....	S8
13. PL spectrum of before and after the B-phase was treated with laser. ....	S8
14. The powder XRD pattern of the G-phase calculated from its crystallographic data and that of after the B-phase was treated with laser. ....	S9
15. Reference . ....	S9

## 1. Synthesis of CN-DSB



Scheme S1. The synthetic scheme

CN-DSB was synthesized according to the procedure shown in Scheme S1.<sup>[1]</sup> All chemicals were purchased commercially, and used without further purification. The mixture of benzaldehyde (0.102 ml, 2 mmol) and 1,4-phenylenediacetonitrile (156.2 mg, 1 mmol) in tert-butyl alcohol (10 mL) was stirred at 46 °C for 30 min. Then, potassium tert-butoxide (1 M solution in tetrahydrofuran, 0.25 mL) and tetrabutylammonium hydroxide (TBAH, 1 M solution in methanol, 0.25 mL) were added, and stirred for 20 minutes. The resulting precipitate was filtered and purified by column chromatography using dichloromethane as an eluent. 1-BCPEB powder (203 mg) was obtained in yield of 60% by evaporated the solvent. <sup>1</sup>H NMR (CDCl<sub>3</sub>) δ [ppm]: 7.94 – 7.92 (d, 4H, Ar-H), 7.78 (s, 4H, Ar-H), 7.62 (s, 2H, Vinyl-H), 7.52 – 7.46 (m, 6H, Ar-H).

## 2. Photograph of CN-DSB crystals in the growth tube

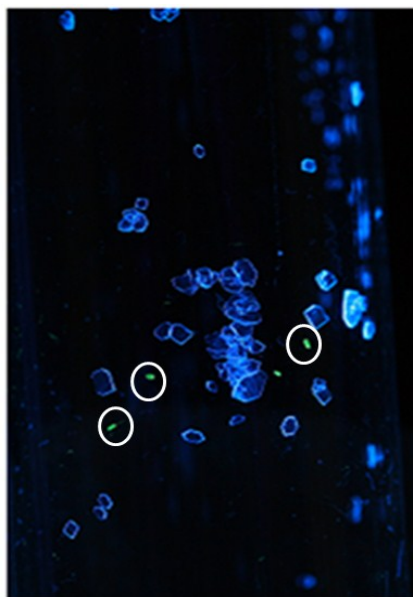


Figure S1. Photograph of CN-DSB crystals in the growth tube under UV light (365 nm). The vast majority of the product through solvent diffusion method is B-phase and just a few piece of G-phase (marked by white circles) is formed simultaneously. As CN-DSB crystal grow from solution, chlorobenzene is used as good solvent. Several days after slowly diffusing vapor poor solvent (petroleum ether) into dilute solution of CN-DSB yields B-phase and G-phase.

### 3. PL spectra of blue and green CN-DSB crystal

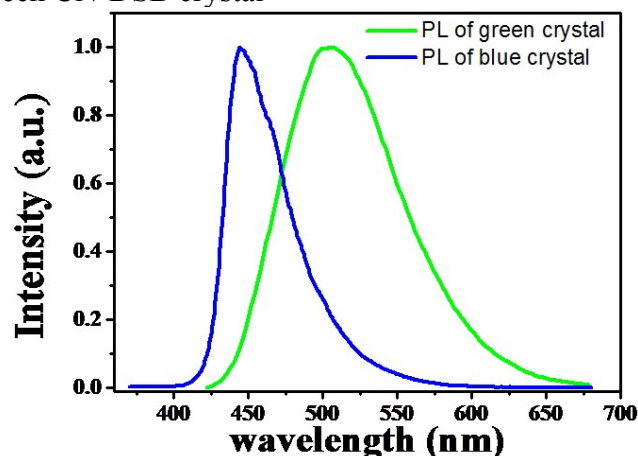


Figure S2. Photoluminescence spectra of blue and green CN-DSB crystal.

### 4. Crystal data and structure refinement

Table S1: Crystal data and structure refinement for two kinds of CN-DSB crystal.

Compound reference	blue CN-DSB crystal	green CN-DSB crystal
Chemical formula	$C_{24}H_{16}N_2$	$C_{24}H_{16}N_2$
Formula Mass	332.39	332.39
Crystal system	Orthorhombic	Monoclinic
$a/\text{\AA}$	6.8410(14)	26.930(6)
$b/\text{\AA}$	7.3130(15)	6.9117(14)
$c/\text{\AA}$	35.529(7)	9.772(2)
$\alpha/^\circ$	90.00	90.00
$\beta/^\circ$	90.00	100.45(3)
$\gamma/^\circ$	90.00	90.00
Unit cell volume/ $\text{\AA}^3$	1777.5(6)	1788.7(7)
Temperature/K	293(2)	293(2)
Space group	$Pbca$	$P2/c$
No. of formula units per unit cell, $Z$	4	4
No. of reflections measured	15707	13195
No. of independent reflections	2018	3106
$R_{int}$	0.0853	0.0551
Final $R_I$ values ( $I > 2\sigma(I)$ )	0.0565	0.0924
Final $wR(F^2)$ values ( $I > 2\sigma(I)$ )	0.1290	0.3063
Final $R_I$ values (all data)	0.0916	0.1382
Final $wR(F^2)$ values (all data)	0.1489	0.3333
CCDC number	892284	892287

## 5. Discussion on PL spectra of blue CN-DSB crystal as increasing the pressure

Lots of works have been done to improve the fluorescence quantum yield ( $\Phi_f$ ) of distyrylbenzene (DSB) through modifying the DSB molecular structure to reduce pi-pi overlap (excited state coupling).<sup>[2]</sup> It is truly that the B-phase has higher  $\Phi_f$  than G-phase has at ambient pressure (there are 75% and 43%, respectively). In this work, the photoluminescence spectra were detected on the surface of the CN-DSB crystal. Due to high crystalline quality, the B-phase CN-DSB crystal exhibiting optical wave guided emission behavior.<sup>[3]</sup> So the signal has been detected was just a part of the photoluminescence, most of the light has emitted from the edge of the crystal. But the G-phase becomes opaque losing optical wave guided emission property, and the light emits is homogenous. Considering the absolute value of G-phase's  $\Phi_f$  is not low, so it is possible that detected emission intensity increased when the B-phase converted to the G-Phase.

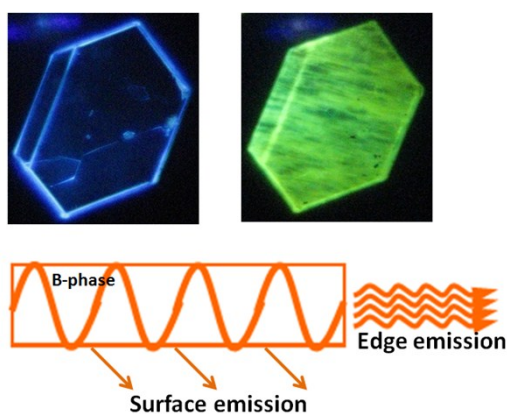


Figure S3. Images of the CN-DSB crystal in a diamond anvil cell (DAC) excited by laser ( $\lambda = 405$  nm) and scheme of optical wave guided emission behavior in B-phase.

6. PL spectra of blue CN-DSB crystal as decreasing the pressure

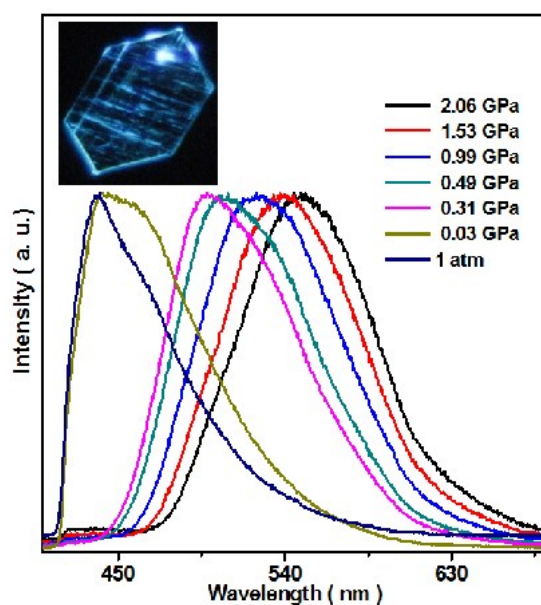


Figure S4. The PL spectra of blue CN-DSB crystal as decreasing the pressure. Insert: Images of CN-DSB crystal in DAC excited by laser ( $\lambda=405$  nm) after released pressure.

7. In situ angle dispersive X-ray diffraction (ADXRD) patterns at varied pressures.

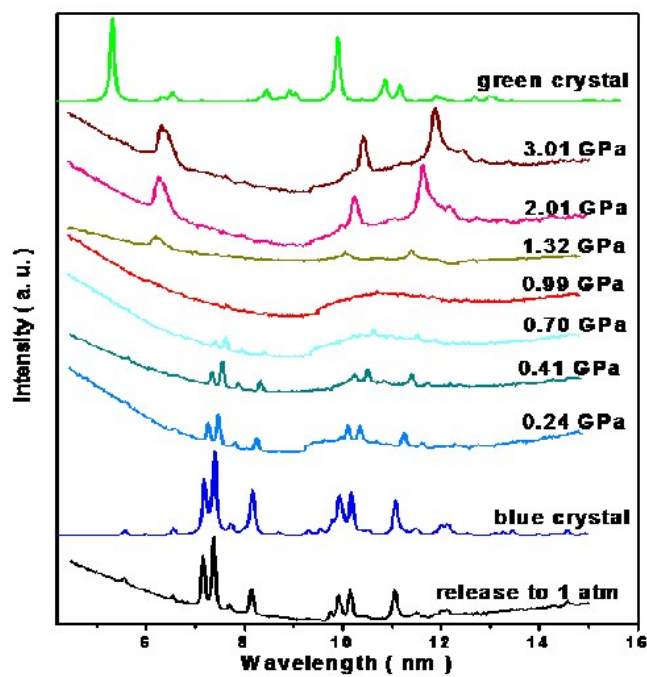


Figure S5. The in situ angle dispersive X-ray diffraction (ADXRD) patterns at varied pressures. The blue and green curves represent the simulated powder XRD patterns of the blue crystal and the green crystal calculated from their crystallographic data, respectively.

8. Pressure-dependent of the intensity ratio  $I_{\text{phenyl}} / I_{\text{vinylene}}$

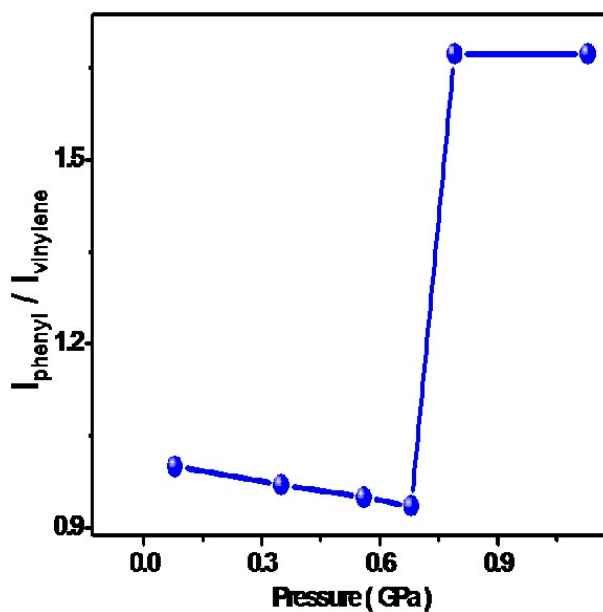


Figure S6. The intensity ratio  $I_{\text{phenyl}} / I_{\text{vinylene}}$  as a function of the pressure.

9. Powder XRD patterns of CN-DSB

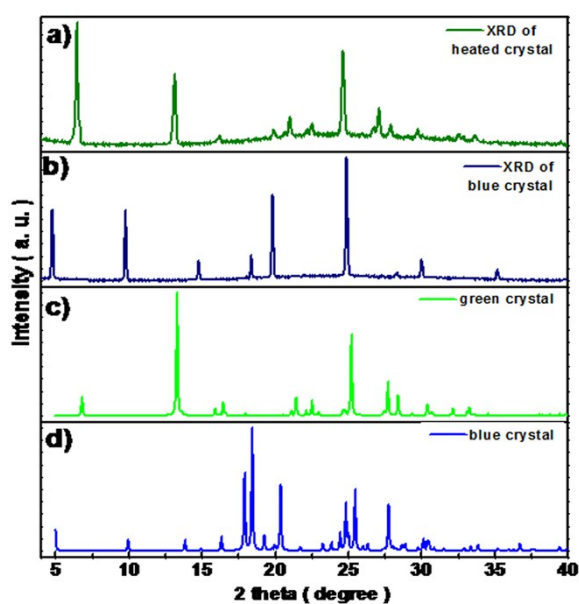


Figure S7. (a, b) Powder XRD patterns of blue crystal after (a) and before (b) heating for 5 minutes at 185°C of CN-DSB solids. (c, d) Simulated powder XRD patterns of the green crystal (c) and the blue crystal (d) calculated from their crystallographic data.

10. FT-IR spectra at room temperature for B-phase and G-phase

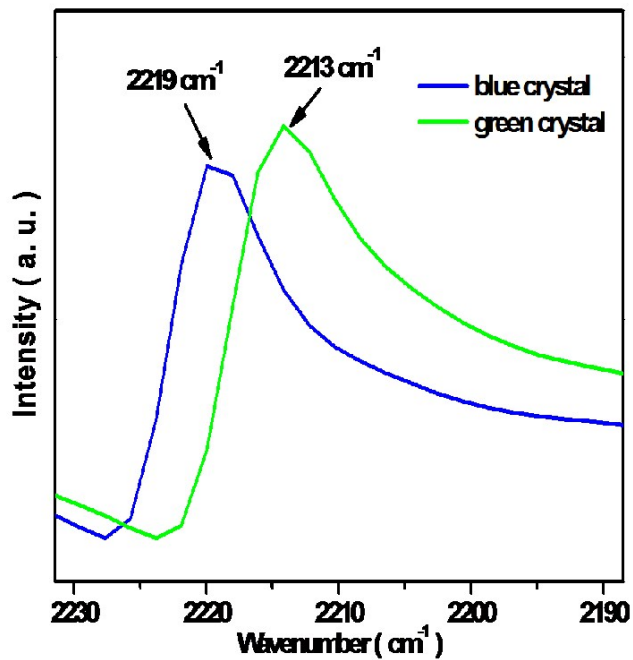


Figure S8. FT-IR spectra at room temperature at 2240-2160  $\text{cm}^{-1}$  region for B-phase and G-phase.

11. Schematic illustration for the FsLDW fabrication of raster

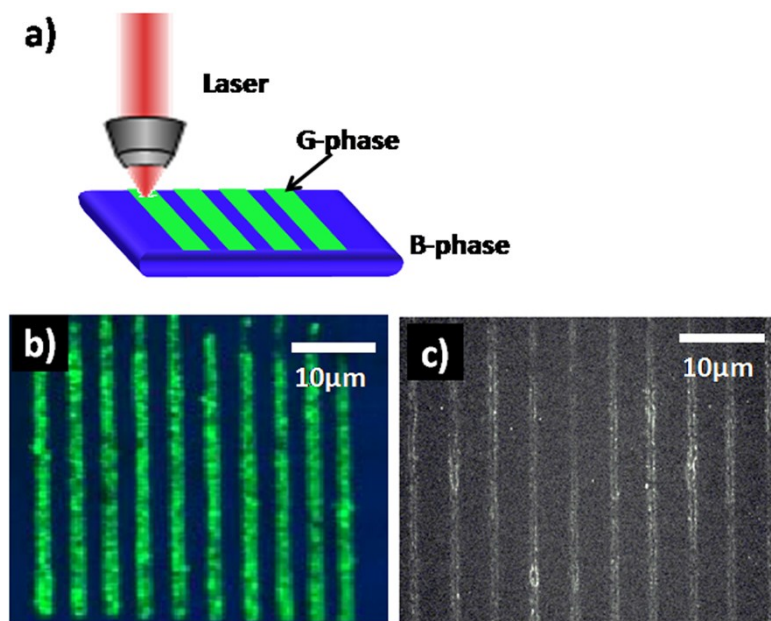


Figure S9. (a) Schematic illustration for the FsLDW fabrication of raster on the surface of the B-phase. (b) and (c) Confocal fluorescence microscopy (left) and SEM image (right) of the as-formed raster prepared by FsLDW. Scale bar: 10  $\mu\text{m}$ .

## 12. The details of FsLDW experiment

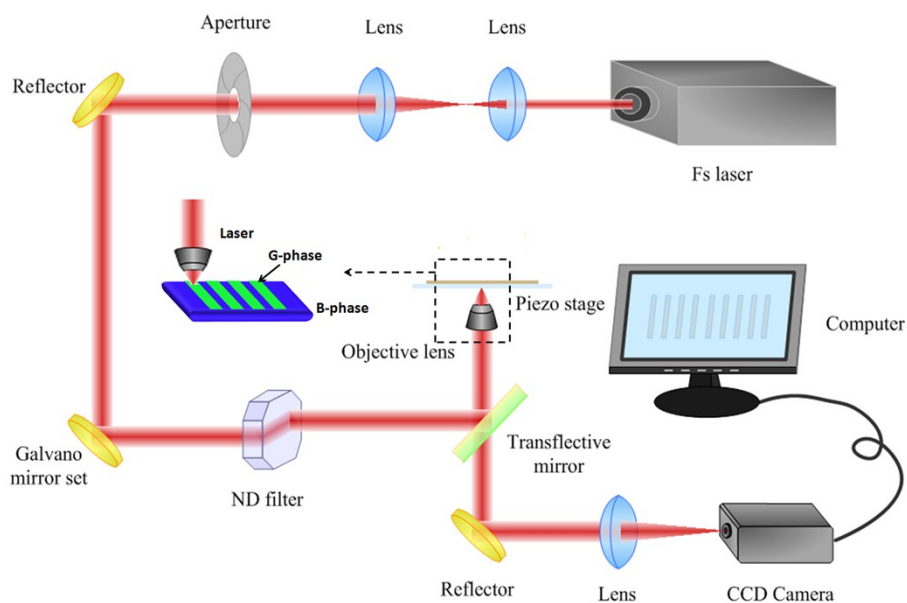


Figure S10. Schematic illustration of the transmittance optical path for the FsLDW fabrication of raster on the surface of the B-phase.

The FsLDW fabrication of raster on the surface of the B-phase was carried out with the setup as shown in Figure S7.<sup>[4]</sup> This system was composed of a femtosecond titanium/sapphire laser (Spectra Physics 3960-X1BB), a piezo stage with a precision of 1 nm (Physik Instrumente P-622.ZCD), and a set of two galvano mirrors. The 3D shape of the raster was designed by using 3Ds Max and then the designs were converted into computer processing programs. The beam from the femtosecond laser (80 MHz repetition

rate, 120 fs pulse width, 780 nm central wavelength, power density  $35 \text{ mW } \mu\text{m}^{-2}$ .) was tightly focused by a high-numerical-aperture (NA=1.40) oilimmersion objective lens (100 $\times$ ). The horizontal and vertical scanning movements of the focused laser spot were achieved simultaneously by the two-galvano-mirror set and the piezo stage.<sup>[5]</sup>

13. PL spectrum of before and after the B-phase was treated with laser

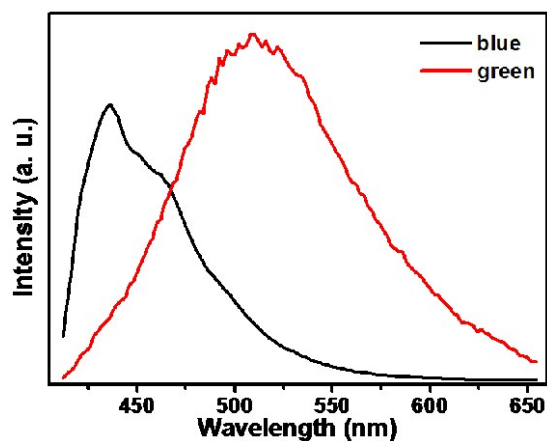


Figure S11. PL spectrum of before and after the B-phase was treated with laser tested by confocal fluorescence microscopy

14. The powder XRD pattern of the G-phase calculated from its crystallographic data and that of after the B-phase was treated with laser.

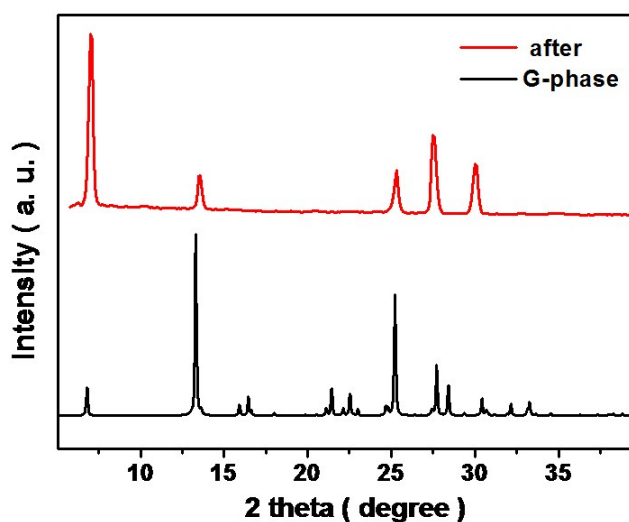


Figure S12. Top: The powder XRD pattern of the G-phase calculated from its crystallographic data. Bottom: the XRD pattern of after the B-phase was treated with laser.

## 15. Reference

- [1] F. J. Lange, M. Leuze, M. Hanack, *J. Phys. Org. Chem.* 2001, **14**, 474.
- [2] (a) S. J. Yoon, S. Y. Park, *J. Mater. Chem.* 2011, **21**, 8338; (b) S. J. Yoon, J. W. Chung, J. Gierschner, K. S. Kim, M. G. Choi, D. Kim, S. Y. Park, *J. Am. Chem. Soc.* 2010, **132**, 13675; (c) S. J. Yoon, S. Y. Park, *J. Mater. Chem.* 2011, **21**, 8338; (d) J. Gierschner, M. Ehni, H.-J. Egelhaaf, B. M. Medina, D. Beljonne, H. Benmansour, G. C. Bazan, *J. Chem. Phys.* 2005, **123**, 144914.
- [3] (a) Y. X. Xu, H. Y. Zhang, F. Li, F. Z. Shen, H. Wang, X. J. Li, Y. Yu, Y. G. Ma, *J. Mater. Chem.* 2012, **22**, 1592; (b) Y. P. Li, F. Z. Shen, H. Wang, F. He, Z. Q. Xie, H. Y. Zhang, Z. M. Wang, L. L. Liu, F. Li, M. Hanif, L. Ye and Y. G. Ma, *Chem. mater.* **2008**, **20**, 7312; (c) M. Ichikawa, R. Hibino, M. Inoue, T. Haritani, S. Hotta, T. Koyama, Y. Taniguchi, *Adv. Mater.* **2003**, **15**, 213.
- [4] Y. L. Sun, W. F. Dong, R. Z. Yang, X. Meng, L. Zhang, Q. D. Chen, H. B. Sun, *Angew. Chem. Int. Ed.* 2012, **51**, 1558.
- [5] a) Q. D. Chen, D. Wu, L. G. Niu, J. Wang, X. F. Lin, H. Xia, H. B. Sun, *Appl. Phys. Lett.* 2007, **91**, 171105; b) D. Wu, L. G. Niu, Q. D. Chen, R. Wang, H. B. Sun, *Opt. Lett.* 2008, **33**, 2913.